EUROGRAPHICS '99 / P. Brunet and R. Scopigno
(Guest Editors)

Volume 18 (1999), Number 3

Compact Metallic Reflectance Models

László Neumann, Attila Neumann, László Szirmay-Kalos

Department of Control Engineering and Information Technology,
Technical University of Budapest,
Budapest, Műegyetem rkp. 11, H-1111, HUNGARY
Email: szirmay@fsz.bme.hu, neumann@mail.datanet.hu

Abstract

The paper presents simple, physically plausible, but not physically based reflectance models for metals and other specular materials. So far there has been no metallic BRDF model that is easy to compute, suitable for fast importance sampling and is physically plausible. This gap is filled by appropriate modifications of the Phong, Blinn and the Ward models. The Phong and the Blinn models are known not to have metallic characteristics. On the other hand, this paper also shows that the Cook-Torrance and the Ward models are not physically plausible, because of their behavior at grazing angles. We also compare the previous and the newly proposed models. Finally, the generated images demonstrate how the metallic impression can be provided by the new models.

Keywords: Reflectance function, BRDF representation, metal models, mirror, albedo function, importance sampling

1. Introduction

The most famous model that can describe specular materials was proposed by Phong[18] and improved by Blinn[3]. This model does not have physical interpretation but is only a mathematical construction. Since the original form violates physics, its corrected version [9, 14] is preferred in global illumination algorithms.

The first model that has physical base was proposed by Torrance and Sparrow [23], which was applied in rendering algorithms in [4]. Later, He, Torrance et. al. [7] introduced another model that even more accurately represented the underlying physical phenomena [2]. These models are not suitable for *importance sampling* since it would require the integration and inversion of the probability density functions that are expected to be proportional to the BRDF multiplied by the cosine of the angle between the direction and the surface normal. Not only is it impossible to compute the required integral and inversion analytically, but even the calculation of BRDF values requires significant computational effort for these physically based models (table 5). Ward[24] and Schlick[20, 21] presented simplified versions of the Cook-Torrance model that are suitable for importance sampling.

In their recent paper Lafortune et. al. approximated a non-linear, metallic BRDF by the combination of modified Phong models [12]. The resulting BRDF is simple, but this approach requires a great number of elementary terms to sufficiently represent highly specular materials. Another drawback of this method is that the directional diffuse part of the BRDF is always bounded for grazing angles.

Radiosity and Monte-Carlo ray-tracing rendering algorithms usually assume that the BRDFs do not violate physics. Such shading models must satisfy both reciprocity and energy balance, and are called *physically plausible* [14].

Reciprocity that was recognized by Helmholtz is the symmetry property of the BRDF (f_r, $[\mathrm{sr}^{-1}]$), which is defined by the following equation [15]:

$$f_r(\vec{L}, \vec{V}) = f_r(\vec{V}, \vec{L}), \tag{1}$$

where $\vec{L}$ is the unit vector pointing towards the incoming light and unit vector $\vec{V}$ defines the viewing direction. Reciprocity is important because it allows for the backward tracing of the light as happens in ray-tracing algorithms.

Suppose that the surface is illuminated by a beam from direction $\vec{L}$. *Energy balance* means that the *albedo*, that is the fraction of the total reflected power cannot be greater

© The Eurographics Association and Blackwell Publishers 1999. Published by Blackwell Publishers, 108 Cowley Road, Oxford OX4 1JF, UK and 350 Main Street, Malden, MA 02148, USA.

than 1:

$$a(\vec{L}) = \int_{\Omega} f_r(\vec{L},\vec{V}) \cdot \cos\Theta_{\vec{V}} \, d\omega_{\vec{V}} \leq 1. \qquad (2)$$

Energy balance makes the linear operator of the rendering equation a contraction, which is required by iterative and random walk methods to converge to the solution.

For the representation of metals, there has been no compact, physically plausible model so far that is suitable for importance sampling, good for highly specular materials and can give back the mirror as the limit case. This paper intends to fill this gap.

2. Metals and Phong-type models

2.1. Properties of metals and mirrors

Metals have several important properties:

- Their diffuse reflectance is usually negligible.
- The color reflected off the metals is determined by the Fresnel function. Due to the angle dependence of the Fresnel function, this color fades at grazing angles.
- If the surface roughness goes to zero, metals become shinier and converge to the *ideal mirror*. The reflectance function of the ideal mirror is $\delta \cdot F(\Theta)/\cos\Theta_{\vec{L}}$, where δ is the Dirac-delta, F is the Fresnel function and $\Theta_{\vec{L}}$ is the incident angle. If the Fresnel term of the material is 1, then an ideal mirror would reflect all energy independently of the illumination, that is the albedo is 1 and the reflected radiance is equal to the corresponding input radiance. At directions other than the reflection direction, the radiance is zero. As the material properties converge to that of the ideal mirror, both the *energy reflectivity* (albedo) and the *radiance reflectivity* (BRDF) are expected to converge to the corresponding functions of the ideal mirror.
- The BRDF function of metals has $1/\cos\Theta_{\vec{L}}$ characteristics that can compensate for the $\cos\Theta_{\vec{L}}$ factor of the irradiance when computing the reflected radiance.
- For great incident angles, the peak of the reflection lobe (so called off-specular peak) occurs at an angle greater than the angle of incidence.

When the new models are compared to the Phong and the Blinn models, these properties are examined. We shall conclude that the new models meet all but the last requirements. This means that instead of the deep physical analysis using, for example, the Maxwell equations, we justify the metallic appearance by checking several characteristic features.

Let us consider the specular part of the physically plausible versions of the Phong and the Blinn models[14]. Using the widely accepted notations where $\vec{R}$ is the mirror direction of $\vec{L}$, $\vec{N}$ is the unit normal vector, and $\vec{H}$ is the halfway unit vector between $\vec{L}$ and the view vector $\vec{V}$, the Phong and Blinn models are defined as the nth power of the dot products $(\vec{R}\cdot\vec{V})$ and $(\vec{N}\cdot\vec{H})$, respectively. For large n values the BRDF gets highly specular. However, these models cannot provide metallic or mirror looking since as the incident angle grows towards the grazing angle, the ratio of the total reflected and incident powers as well as the output radiance decrease. If n goes to infinity, then the reflected radiance and the albedo converges to zero for 90 degree incident angle since in this limit case the albedo follows the cosine function. Intuitively, the decrease of the radiance means that if we look at a "Phong-mirror", then the image reflected in the mirror gets darker for greater reflection angles.

2.2. The new metallic models

This section discusses a construction method which preserves the reciprocity and the energy balance of the BRDF, but solves the mentioned problems of Phong-type models. The new model is empirical, that is a pure mathematical construction, whose validity is guaranteed by satisfying the basic properties of metals.

The reflected radiance of the physically plausible Phong model follows the $\cos^n\alpha \cdot \cos\Theta_{\vec{L}}$ function, where the $\cos\Theta_{\vec{L}}$ factor is responsible for making the Phong mirror dark for greater reflection angles. In order to eliminate this undesired behavior of the Phong model, it must be compensated by an $1/\cos\Theta_{\vec{L}}$ factor. However, if we multiplied the specular part of the reciprocal Phong model [13] by $1/\cos\Theta_{\vec{L}}$, then we would get back the original, non-reciprocal Phong [18] expression. Obviously, we have to find a symmetric function of $\vec{L}$ and $\vec{V}$, which gives $1/\cos\Theta_{\vec{L}}$ value only in the $\vec{L}=\vec{V}$ case.

We have examined several different alternatives. If we multiplied the Phong BRDF with $1/(\cos\Theta_{\vec{L}}\cdot\cos\Theta_{\vec{V}})$, then the radiance would be unacceptably high around the reflection direction at grazing angles and the energy balance could not be preserved. We can come to the same conclusion with $1/\sqrt{(\cos\Theta_{\vec{L}}\cdot\cos\Theta_{\vec{V}})}$ [24] correction factor as well.

The $2/(\cos\Theta_{\vec{L}}+\cos\Theta_{\vec{V}})$, which can also be called as the "plus-model", has unrealistic supermetal features. It means that it relfects two times greater radiance at grazing angles than at orthogonal illumination (figures 1 and 2).

Finally, only the $1/\max(\cos\Theta_{\vec{L}},\cos\Theta_{\vec{V}})$ function has been found appropriate from the set of simple $\vec{L},\vec{V}$ symmetric functions. The fact that its derivative is not continuous has no visible artifacts, similarly to the Cook-Torrance model. Let the minimum of the incident and the viewing angles be $\Theta_{\min}$:

$$\Theta_{\min} = \min(\Theta_{\vec{L}},\Theta_{\vec{V}}). \qquad (3)$$

Then the proposed correction term is

$$\frac{1}{\cos\Theta_{\min}} = \frac{1}{\max(\cos\Theta_{\vec{L}},\cos\Theta_{\vec{V}})}. \qquad (4)$$

Let $\cos\alpha = (\vec{R}\cdot\vec{V})^+$ where $(\vec{R}\cdot\vec{V})^+ = (\vec{R}\cdot\vec{V})$ if $(\vec{R}\cdot\vec{V}) \geq 0$

© The Eurographics Association and Blackwell Publishers 1999.

	recip. Phong	recip. Blinn	Cook-Torrance	Ward	He-Torrance
rel. computation time	1	1.8	4.2	4.0	320
metallic	N	N	Y	Y	Y
physically plausible	Y	Y	N	N	Y
physically based	N	N	Y	N	Y
off-specular peak	N	N	Y	N	Y
importance sampling	Y	Y	N	Y	N

Table 1: *Comparison of existing BRDF models (the running-time measurements used Heckbert's BRDF viewer[8])*

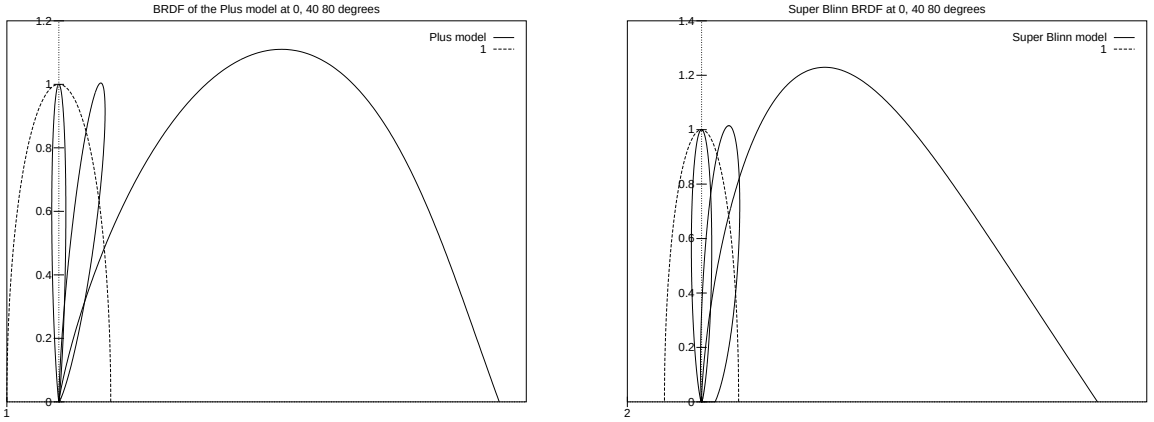

Figure 1: *The BRDFs of the plus-Phong and the plus-Blinn models ($n = 100$)*

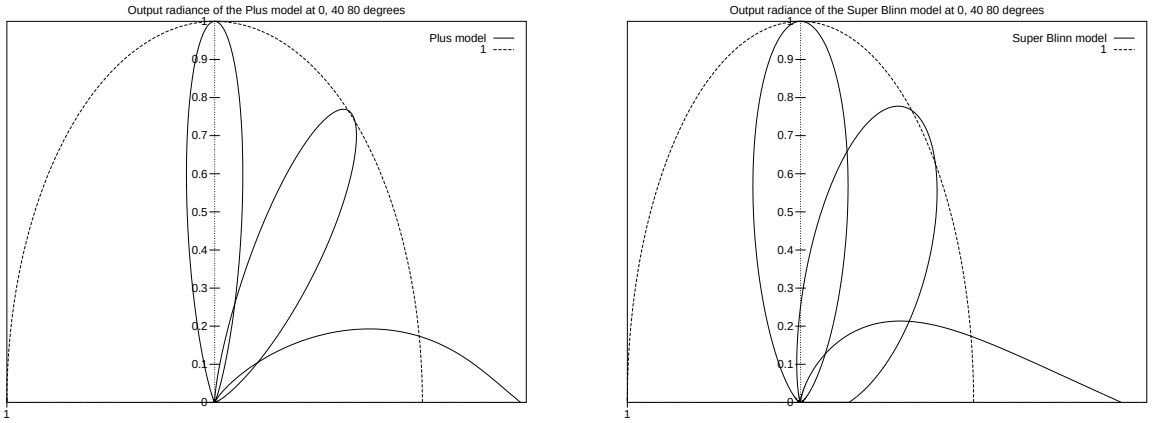

Figure 2: *The output radiance of the plus-Phong and the plus-Blinn models ($n = 20$)*

© The Eurographics Association and Blackwell Publishers 1999.

and 0 otherwise. The BRDF of the reciprocal Phong model is

$$f_{r,\text{Phong}}(\vec{L},\vec{V}) = c_n \cdot \cos^n \alpha \tag{5}$$

where c_n is a scalar parameter. Lafortune [13] has shown that

$$c_n \leq \frac{n+2}{2\pi} \tag{6}$$

must hold in order for the model to preserve energy balance.

The new reciprocal BRDF of the *stretched Phong model* is

$$\boxed{f_r(\vec{L},\vec{V}) = c_n \cdot \frac{\cos^n \alpha}{\cos \Theta_{\min}}.} \tag{7}$$

This model meets the mentioned requirements and really provides metallic impression as we demonstrate it later.

Since the reflection vector $\vec{R}$ is

$$\vec{R} = 2(\vec{N}\cdot\vec{L})\vec{N} - \vec{L}, \tag{8}$$

the formula to compute $(\vec{R}\cdot\vec{V})$ can be expressed as

$$(\vec{R}\cdot\vec{V}) = (2(\vec{N}\cdot\vec{L})\vec{N} - \vec{L})\cdot\vec{V} = 2(\vec{N}\cdot\vec{L})(\vec{N}\cdot\vec{V}) - (\vec{L}\cdot\vec{V}). \tag{9}$$

Substituting this into equation 7, we can obtain the following formula for the new BRDF:

$$f_r(\vec{L},\vec{V}) = c_n \cdot \frac{[(2(\vec{N}\cdot\vec{L})(\vec{N}\cdot\vec{V}) - (\vec{L}\cdot\vec{V}))^+]^n}{\max((\vec{N}\cdot\vec{L}),(\vec{N}\cdot\vec{V}))}. \tag{10}$$

The albedo function of the new model can be computed from the Phong BRDF as the sum of the following two integrals:

$$a(\vec{L}) = \int_{\Omega((\vec{N}\cdot\vec{L})<(\vec{N}\cdot\vec{V}))} f_{r,\text{Phong}}(\vec{L},\vec{V})\, d\omega_{\vec{V}} + \int_{\Omega((\vec{N}\cdot\vec{L})\geq(\vec{N}\cdot\vec{V}))} f_{r,\text{Phong}}(\vec{L},\vec{V}) \cdot \frac{(\vec{N}\cdot\vec{V})}{(\vec{N}\cdot\vec{L})}\, d\omega_{\vec{V}}. \tag{11}$$

Analyzing the albedo functions we can come to the conclusion that the c_n constant of inequality 6 is also good for the new model. More precisely, the albedo of the BRDF of equation 7 has only a negligible overshooting where it exceeds value 1 if $n \geq 1$. The overshooting occurs at small incident angles where $\vec{L}$ is close to $\vec{N}$.

Below the arbitrarily selected $n = 1$ minimum, the c_n value should be decreased in order to preserve energy balance, which would shift the maximum of the albedo function and the BRDF from the perpendicular incident direction. For example, if $n = 1$, then the maximum c_n constant would result in 0.0003 maximum overshooting at 13 degrees. For higher n values, the overshooting is negligible.

Figure 3 shows the albedo functions for different n values. We can see that in the limit case the albedo converges to constant 1, which is the albedo of the ideal mirror.

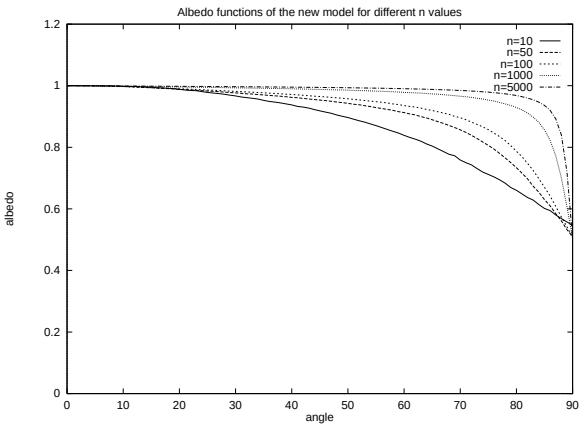

Figure 3: *Albedo functions of the stretched model for different n values*

2.3. Transition from the Phong model to the new model: p-model

Using a $p \in [0,1]$ parameter, a continuous transition can be developed between the reciprocal Phong model defined by equation 5 and the new metallic model, as follows:

$$f_r(\vec{L},\vec{V}) = c_n \cdot \frac{\cos^n \alpha}{\cos^p \Theta_{\min}}, \qquad 0 \leq p \leq 1. \tag{12}$$

Let us call this formula the p-model. If $n \geq 1$, then the maximum of the multiplicative factor c_n is as shown in equation 6 for any $p \in [0,1]$.

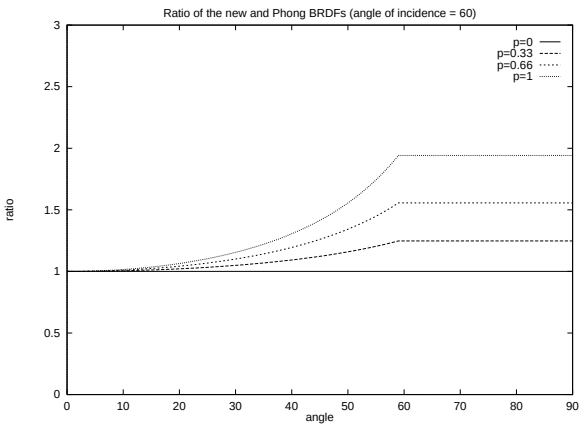

Figure 4: *Ratio of the p-model and the Phong BRDFs for different viewing angles*

Figure 4 shows the ratio of the BRDFs of the p-model and the Phong model for different viewing angles $\Theta_{\vec{V}}$ and for different transition parameters p. The case of $p = 0$ represents the reciprocal Phong model, while the case of $p = 1$ means the new metallic model.

© The Eurographics Association and Blackwell Publishers 1999.

2.4. The metallic properties of the stretched Phong model

This section examines the properties of the new model.

Supposing that the Fresnel term is 1 (for silver this is practically true), the albedos of the Phong, He-Torrance, Cook-Torrance, Ward and the stretched Phong models are shown in figure 5. Note that the Cook-Torrance and the Ward models diverge at grazing angles (for the formal proof please refer to[16]), while the Phong, He-Torrance and Ward BRDFs badly decrease for greater incident angles. The stretched model converges to a value that is not lower than 0.5 for grazing angles.

The maximum of the stretched Phong BRDF is always at the mirror direction $\vec{R}$ and its value is $c_n/\cos\Theta_{\vec{L}}$ for any n, while the maximum of the Phong model is always c_n.

Figure 6 compares the normalized BRDF functions of the Phong and the stretched Phong models for 0, 40 and 80 degree incident angles (normalization scales the BRDF to be 1 at 0 incident angle).

It is also worth examining the output radiance assuming a single point-like lightsource of intensity 4π at distance 1 in direction $\vec{L}$. In this case the irradiance is $\cos\Theta_{\vec{L}}$. The output radiances of the Phong and the stretched models at different incident directions are shown in figure 7. This figure demonstrates the earlier statement that the "Phong-mirror" gets darker for greater incident angles, but the stretched model eliminates this artifact.

2.4.1. Ideal mirror

The new model gives back the normalized BRDF of the ideal mirror for $n \to \infty$, which is $1/\cos\Theta_{\vec{L}}$. The output radiance is $L^{\text{out}}(\vec{V}) = L^{\text{in}}(\vec{L})$ if $\vec{V} = \vec{L}$ and 0 otherwise.

Note that the new model can arbitrarily approximate the ideal mirror. Selecting n in an appropriate way (e.g. $n = 10^4 \ldots 10^8$), realistic, glossy mirrors can easily be generated. Using, for example, distributed ray-tracing, the mirrors do not require a special case. On the other hand, realistic, "almost-ideal" mirrors can also be handled.

2.4.2. Off-specular peak

The new model does not provide off-specular peak which can be quite significant for highly polished metals. For example, when the He-Torrance model was fitted, it was realized [11] that at 75° incident angle the off-specular peak can be 1.6 times greater than the radiance at the mirror direction. Although it is difficult to decide how important the off-specular peak is in providing metallic impression, experience gained with other models [24] show that this effect is not significant.

3. Generalizations of the new model

3.1. Retro-reflective materials

The proposed model can easily be generalized to provide a *retro-reflective* BRDF which has the maximum at the direction of the incident illumination. Practical examples of retro-reflective objects are a projection screen, a traffic sign, etc. For retro-reflective materials, mirror direction vector $\vec{R}$ should be replaced by the illumination direction $\vec{L}$. The BRDF formula can be simplified to the following form:

$$f_r(\vec{L},\vec{V}) = c_n \cdot \frac{[(\vec{L}\cdot\vec{V})^+]^n}{\max((\vec{N}\cdot\vec{L}),(\vec{N}\cdot\vec{V}))}. \qquad (13)$$

The maximum value of c_n is as defined in equation 6.

3.2. Anisotropic materials

Lafortune et. al. [12] introduced the anisotropic generalization of the Phong model as:

$$f_r(\vec{L},\vec{V}) = C_{\max}\cdot(C_x(R_xV_x)+C_y(R_yV_y)+C_z(R_zV_z))^n =$$

$$C_{\max}\cdot[(\vec{R}\cdot\vec{V})_M]^n, \qquad (14)$$

where $(\vec{R}\cdot\vec{V})_M = \vec{R}^{\mathrm{T}}M\vec{V}$ is a special dot product containing also a multiplication with diagonal matrix M. The values at the diagonal of M are C_x, C_y and C_z, respectively.

As for the original Phong model, the anisotropic generalization can also be normalized with p-th power of the maximum of the dot products $(\vec{N}\cdot\vec{L})$, $(\vec{N}\cdot\vec{V})$, thus we can obtain:

$$f_r(\vec{L},\vec{V}) = C_{\max}\cdot\frac{[(\vec{R}\cdot\vec{V})_M]^n}{\max((\vec{N}\cdot\vec{L}),(\vec{N}\cdot\vec{V}))^p}. \qquad (15)$$

This model is able to approximate metals even with a single term, or by fewer terms than required by Lafortune's approximation. The general formula containing a combination of several terms is:

$$f_r(\vec{L},\vec{V}) = \sum_i C_i\cdot\frac{[(\vec{R}\cdot\vec{V})_{M_i}]^{n_i}}{\max((\vec{N}\cdot\vec{L}),(\vec{N}\cdot\vec{V}))^{p_i}}. \qquad (16)$$

In the original form of the Lafortune's model, highly specular materials require very many terms (for example, if the RMS slope is less than 0.02, the number of terms may exceed a hundred). The new model can significantly reduce this number.

4. Importance sampling

Importance sampling is an effective technique to reduce the variance of Monte-Carlo algorithms. It requires the generation of random samples according to a probability density which is proportional, or at least approximately proportional to the integrand.

In order to generate the output radiance $L^{\text{out}}(\vec{V})$ from the

© The Eurographics Association and Blackwell Publishers 1999.

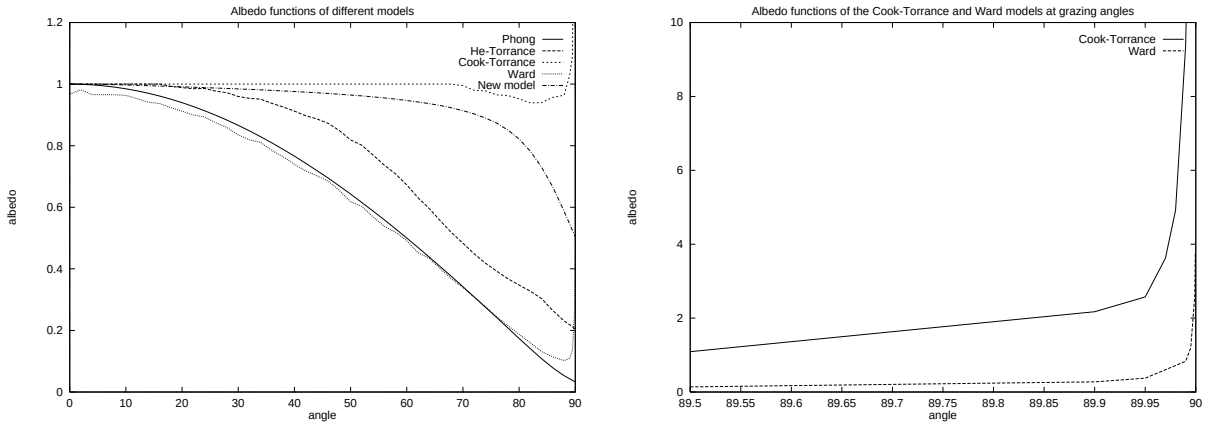

Figure 5: *Albedo functions of the Phong ($n = 150$), stretched Phong ($n = 150$), Cook-Torrance ($m = 0.1$), Ward ($m = 0.1$) and He-Torrance ($\sigma_0 = 0.1,\ \tau = 1.7$) models*

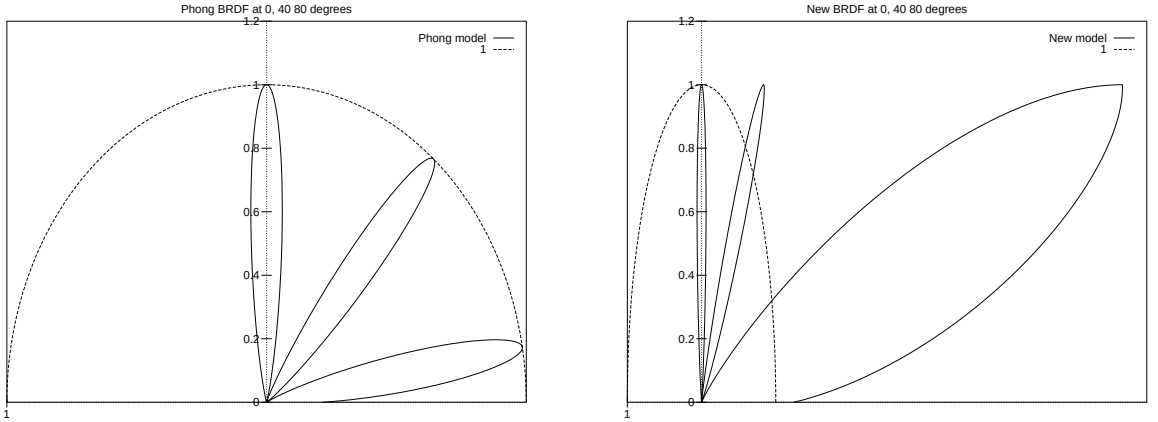

Figure 6: *Comparison of the BRDFs of the original and the stretched Phong models ($n = 100$)*

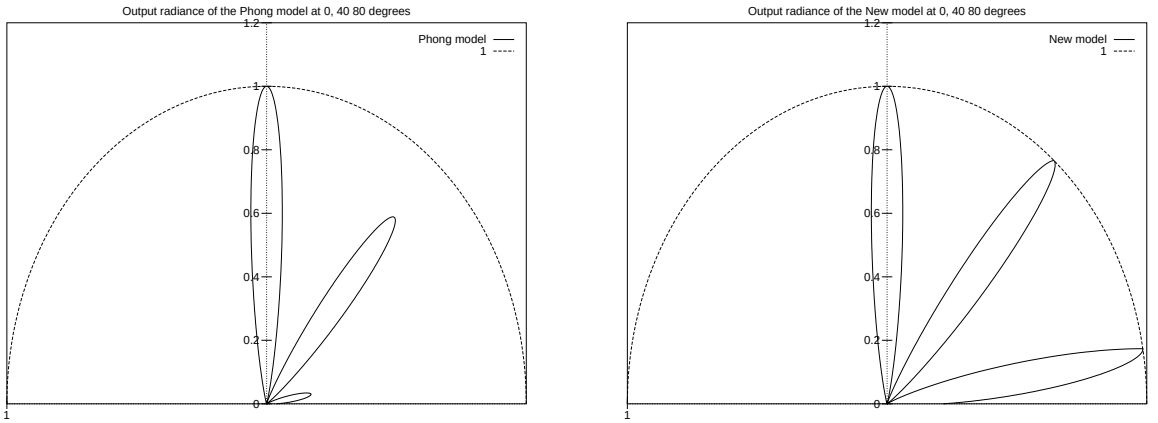

Figure 7: *Comparison of the output radiances of the original and the stretched Phong models ($n = 100$)*

© The Eurographics Association and Blackwell Publishers 1999.

incident illumination $L^{\text{in}}(\vec{L})$ ($\vec{L} \in \Omega$) in Monte-Carlo ray-tracing, the following integral should be evaluated:

$$L^{\text{out}}(\vec{V}) = \int_{\Omega} L^{\text{in}}(\vec{L}) \cdot f_r(\vec{L},\vec{V}) \cdot \cos\Theta_{\vec{L}}\, d\omega_{\vec{L}}. \qquad (17)$$

If directions $\vec{L}_1, \vec{L}_2, \ldots, \vec{L}_M$ are sampled following probability density $p(\vec{L})$, then the Monte-Carlo estimate of this integral is:

$$L^{\text{out}}(\vec{V}) \approx \frac{1}{M} \cdot \sum_{m=1}^{M} L^{\text{in}}(\vec{L}_m) \cdot \frac{f_r(\vec{L}_m,\vec{V}) \cdot \cos\Theta_{\vec{L}_m}}{p(\vec{L}_m)}. \qquad (18)$$

According to the concept of *importance sampling*, $p(\vec{L})$ should be approximately proportional to the integrand to minimize the variance of the solution. If no a-priori information is available about L^{in}, then it is assumed to be constant, thus the probability density should be proportional to $f_r(\vec{L},\vec{V}) \cdot \cos\Theta_{\vec{L}}$.

4.1. Importance sampling for the Phong model

For the Phong model where the integrand is

$$L^{\text{in}}(\vec{L}) \cdot c_n \cdot (\vec{V}\cdot\vec{R})^n \cdot \cos\Theta_{\vec{L}} = L^{\text{in}}(\vec{L}) \cdot c_n \cdot \cos^n\alpha \cdot \cos\Theta_{\vec{L}},$$

Lafortune [13] proposed the following probability density:

$$p(\vec{L}) = \frac{n+1}{2\pi} \cdot [(\vec{V}\cdot\vec{R})^+]^n = \frac{n+1}{2\pi} \cdot \cos^n\alpha. \qquad (19)$$

Samples according to this probability density can be generated in the following way. Suppose that we can get (u_m, v_m) samples from a set containing uniformly distributed points in the unit square. Note that this sampling will be used in Monte-Carlo ray-tracing where rays are traced backwards. It means that for a given $\vec{V}$ an appropriate $\vec{L}$ vector should be found, which consists of two steps. In the first step reflection direction $\vec{R}_m$ is found, then $\vec{L}_m$ is generated by mirroring.

In order to find a reflection direction $\vec{R}_m$, angles α_m and ϕ_m in the lobe around $\vec{V}$ is generated:

$$(\alpha_m, \phi_m) = (\arccos u_m^{\frac{1}{n+1}}, 2\pi v_m). \qquad (20)$$

Note that using this formula, the probability density of generating a given direction (α,ϕ) is $\frac{(n+1)}{2\pi}\cos^n\alpha$ which is proportional to the BRDF.

Let us establish a Cartesian coordinate system $\vec{i},\vec{j},\vec{k}$ where $\vec{k} = \vec{V}$, and:

$$\vec{i} = \frac{\vec{V}\times\vec{N}}{|\vec{V}\times\vec{N}|}, \qquad \vec{j} = \vec{i}\times\vec{k}. \qquad (21)$$

Using these unit vectors, the mirror direction $\vec{R}_m$ is:

$$\vec{R}_m = \sin\alpha_m\cdot\cos\phi_m\cdot\vec{i} + \sin\alpha_m\cdot\sin\phi_m\cdot\vec{j} + \cos\alpha_m\cdot\vec{k}. \qquad (22)$$

From the mirror direction the light vector can be derived easily: $\vec{L}_m = ((\vec{N}\cdot\vec{R})_m\vec{N} - \vec{R}_m$. The sampling according to this probability density may generate directions that point into the object ($(\vec{N}\cdot\vec{L})_m < 0$). Thus we should check whether or not the light vector points out of the object ($(\vec{N}\cdot\vec{L})_m \geq 0$) and reject this sample if it does not. This rejection poses no problem since from these directions $L^{\text{in}}(\vec{L}_m)$ is zero, thus these samples would get zero weight.

Summarizing, the Monte-Carlo estimate of the output radiance is

$$L^{\text{out}}(\vec{V}) \approx \frac{1}{M} \cdot \frac{2\pi c_n}{n+1} \cdot \sum_{m=1}^{M} L^{\text{in}}(\vec{L}_m) \cdot \cos\Theta_{\vec{L}_m}. \qquad (23)$$

If c_n is the maximum allowed by inequality 6, then we obtain

$$L^{\text{out}}(\vec{V}) \approx \frac{1}{M} \cdot \frac{n+2}{n+1} \cdot \sum_{m=1}^{M} L^{\text{in}}(\vec{L}_m) \cdot \cos\Theta_{\vec{L}_m}. \qquad (24)$$

The selected probability density is not optimally proportional to the integrand, only with $\cos^n\alpha$. It would be better to find a density that is proportional to $\cos^n\alpha\cdot\cos\Theta_{\vec{L}}$, but it would be quite complicated to implement practically. This simplification reduces the efficiency of the importance sampling, since the ignored $\cos\Theta_{\vec{L}}$ can be arbitrarily small at grazing angles, and its average is only $1/2$.

4.2. Importance sampling for the stretched Phong model

The efficiency of the importance sampling gets higher for the new model, and it will be particularly good at grazing angles. For the new model the integrand is

$$I(\vec{L},\vec{V}) = L^{\text{in}}(\vec{L}) \cdot c_n \cdot \frac{\cos^n\alpha}{\max(\cos\Theta_{\vec{L}}, \cos\Theta_{\vec{V}})} \cdot \cos\Theta_{\vec{L}},$$

which can be simplified if the cases when the incident angle is smaller than the viewing angle ($\cos\Theta_{\vec{L}} \geq \cos\Theta_{\vec{V}}$) and when the incident angle is greater than the viewing angle ($\cos\Theta_{\vec{L}} < \cos\Theta_{\vec{V}}$) are considered separately:

$$I(\vec{L},\vec{V}) = L^{\text{in}}(\vec{L}) \cdot c_n \cdot \cos^n\alpha \quad \text{if } \Theta_{\vec{L}} \leq \Theta_{\vec{V}},$$
$$I(\vec{L},\vec{V}) = L^{\text{in}}(\vec{L}) \cdot c_n \cdot \cos^n\alpha \cdot \frac{\cos\Theta_{\vec{L}}}{\cos\Theta_{\vec{V}}} \quad \text{if } \Theta_{\vec{L}} > \Theta_{\vec{V}}.$$

As for the Phong model, the samples are generated according to $\frac{n+1}{2\pi}\cos^n\alpha$ probability density function. Using the $c_n = (n+2)/2\pi$ substitution, the Monte-Carlo approximation of the integral is:

$$L^{\text{out}}(\vec{V}) \approx \frac{1}{M} \cdot \frac{n+2}{n+1} \cdot$$

$$\left(\sum_{\Theta_{\vec{L}_m} \leq \Theta_{\vec{V}}}^{M} L^{\text{in}}(\vec{L}_m) + \sum_{\Theta_{\vec{L}_m} > \Theta_{\vec{V}}}^{M} L^{\text{in}}(\vec{L}_m) \cdot \frac{\cos\Theta_{\vec{L}_m}}{\cos\Theta_{\vec{V}}} \right). \qquad (25)$$

For large viewing angles the samples will be in the first sum of equation 25. Note that the probability density also compensates for the $\cos\Theta_{\vec{L}}$ factor here, thus this results in

© The Eurographics Association and Blackwell Publishers 1999.

a more effective importance sampling. The larger the viewing angle, the greater the efficiency (even if the probability of the rejected samples approaches 0.5). The worst case of the importance sampling of the new model is at zero degree viewing angle, where the efficiency degrades to that of the sampling of the Phong model, which is fortunately the best here.

4.3. Albedo at grazing angles

Note that for $L^{\text{in}} = 1$ equation 17 gives the albedo function at illumination direction $\vec{V}$, thus the importance sampling can also be used to effectively calculate and tabulate the values of the albedo function.

Equation 25, that calculates the albedo as an expected value, can also be given an intuitive explanation. At 90 degree viewing direction, the weight of sample rays is

$$(n+2)/(n+1).$$

Since the BRDF is symmetric around $\vec{R}$, half of the samples point into the object, and are thus rejected. Consequently, the albedo at 90 degrees is:

$$\tilde{a}(90^\circ) = \frac{n+2}{2(n+1)}. \tag{26}$$

The albedos at grazing angles for $n = 1$, $n = 2$ and $n \to \infty$ are 3/4, 2/3 and 1/2, respectively. Note that for $n \to \infty$ which represents the ideal mirror case, for any $\varepsilon > 0$, $\tilde{a}(90^\circ - \varepsilon) = 1$, thus the new model can really converge to the ideal mirror.

5. Visualization of real materials

5.1. Metals

Metals have negligible diffuse reflectance and their BRDF is proportional to the Fresnel function which is based on a complex and wavelength dependent refraction index κ [5]. The Fresnel function also depends on the incident angle making the highlights colored. The reflected color can be computed as a product of the irradiance and the BRDF, which is usually done at a few discrete wavelengths.

For a single wavelength λ, the new BRDF for metals is:

$$f_r(\vec{L},\vec{V},\lambda) = \frac{n+2}{2\pi} \cdot \frac{\cos^n \alpha}{\cos \Theta_{\min}} \cdot F(\kappa(\lambda), \Theta(\vec{L},\vec{V})), \tag{27}$$

where $\Theta(\vec{L},\vec{V})$ is an appropriate incident angle, which should be a symmetric function of $\vec{L}$ and $\vec{V}$ to make the model reciprocal.

A straightforward selection is the angle of the halfway vector $\vec{H}$. Another alternative is letting $\Theta = \Theta_{\min}$. This alternative gives back the angle of the halfway vector for the mirror direction but for other directions it generates a smaller angle. The largest difference between the angle of the halfway vector and $\Theta_{\min}$ occurs when the lighting is perpendicular to the surface and the viewing direction is parallel to it. Here $\Theta_{\min} = 0$ while the angle of the halfway vector is 45°. Fortunately, the larger variation of Fresnel function is usually closer to 90° than to 0.

If we select $\Theta_{\min}$ to evaluate the Fresnel function, then the resulting BRDF is

$$f_{r,\text{metal}}(\vec{L},\vec{V},\lambda) = \frac{n+2}{2\pi} \cdot \frac{\cos^n \alpha}{\cos \Theta_{\min}} \cdot F(\kappa(\lambda), \Theta_{\min}) =$$

$$\frac{\cos^n \alpha}{g(\Theta_{\min})}, \tag{28}$$

where $g(\Theta_{\min})$ can be tabulated for the considered wavelengths. These tables allow for very fast BRDF evaluation. This computational cost is lower than that of any previously known metallic models.

5.2. Plastics and ceramics

The new model is appropriate not only for metals but also for other materials that have highly specular reflection components, such as for certain plastics and ceramics. The main difference between these materials and metals is that their diffuse component is relevant and the specular part is responsible for the smaller part of the reflected power. For non metals the refraction index is a real number. The highlights can be assumed to be white everywhere not only for greater incident angles.

When rendering plastics, the classical Lambertian model can be applied for the diffuse component, while the specular part can be determined by the new model. Thus the BRDF has two components:

$$f_{r,\text{plastics}}(\vec{L},\vec{V},\lambda) =$$

$$\frac{a_d(\lambda)}{\pi} + a_s \cdot \frac{n+2}{2\pi} \cdot \frac{\cos^n \alpha}{\cos \Theta_{\min}} \cdot F(\kappa(\lambda), \Theta_{\min}), \tag{29}$$

where reflectivity a_d is the albedo of the diffuse component and a_s determines the size of the specular part. In order to make the model conserve energy, $a_s + a_d$ should not exceed 1. In many practical situations it is enough to compute the color on the three primary colors (r,g,b) and the Fresnel function can be assumed to be constant 1. For this simplified case the following plastic model is proposed:

$$f_{r,\text{plastics}}(\vec{L},\vec{V}) = \frac{(r,g,b)}{\pi} + a_s \cdot \frac{n+2}{2\pi} \cdot \frac{\cos^n \alpha}{\cos \Theta_{\min}} \cdot (1,1,1), \tag{30}$$

where r,g,b are the albedos of the diffuse component at the wavelengths of the three primaries, and $a_s \leq 1 - \max(r,g,b)$ should hold. It should be noted that not all non-metal materials can be visualized by this simple BRDF, and more sophisticated plastic models [17] might be required. However, this is a computationally effective model for many practical cases.

© The Eurographics Association and Blackwell Publishers 1999.

6. Reflectance models of $(\vec{N}\cdot\vec{H})$ type

6.1. Blinn model and stretched Blinn models

The Blinn model can be modified similarly as the Phong model was corrected. Recall that the specular part of the original Blinn model [3] is

$$f_{r,\mathrm{Blinn}}(\vec{L},\vec{V}) = C_n\cdot(\vec{N}\cdot\vec{H})^n. \tag{31}$$

The analytical calculation of the C_n constant for integer n values can be found in [1]. The complexity of this calculation is $O(n)$. The problems of this model are similar to that of the Phong model. The reflected radiance and the albedo converges to zero at grazing angles if n goes to infinity.

Similarly to the procedures applied for the Phong model, this model can also be corrected resulting in a *stretched Blinn model*:

$$f_r(\vec{L},\vec{V}) = C_n\cdot\frac{(\vec{N}\cdot\vec{H})^n}{\max((\vec{N}\cdot\vec{L}),(\vec{N}\cdot\vec{V}))}. \tag{32}$$

The C_n constants that can be allowed not to violate energy balance are summarized by table 2.

n	Blinn	Blinn$/\cos\Theta_{\min}$
1	0.350	0.293
2	0.382	0.368
4	0.449	0.449
8	0.592	0.592
16	0.895	0.895
32	1.52	1.52
64	2.79	2.79
128	5.34	5.34
256	10.4	10.4
512	20.6	20.6

Table 2: *The maximum C_n constants for the original and the corrected Blinn models (note that for $n \geq 4$ the original and the stretched Blinn models have practically the same constant)*

6.1.1. Mean albedo

If the irradiance L^{in} is constant in the whole hemisphere, then the ratio of the total reflected power is called the *mean albedo*, which can be obtained as:

$$a_{\mathrm{mean}} = \frac{1}{\pi}\cdot\int_{\Omega} a(\vec{L})\cdot\cos\Theta_{\vec{L}}\, d\omega_{\vec{L}}. \tag{33}$$

For diffuse white materials and for the ideal mirror the mean albedo is 1. Table 3 shows the mean albedo for different models.

n	Phong	$\frac{\text{Phong}}{\cos\Theta_{\min}}$	Blinn	$\frac{\text{Blinn}}{\cos\Theta_{\min}}$
1	0.737	0.934	0.879	0.941
2	0.708	0.902	0.800	0.952
4	0.688	0.887	0.706	0.863
8	0.676	0.888	0.620	0.748
16	0.670	0.901	0.562	0.679
32	0.668	0.919	0.531	0.648
64	0.667	0.937	0.516	0.639
128	0.667	0.953	0.508	0.640
256	0.667	0.966	0.504	0.644
512	0.667	0.975	0.502	0.649
∞	0.5	1	0.5	1

Table 3: *Mean albedo values of different models*

The proposed correction by $1/\cos\Theta_{\min}$ has "pumped-up" the mean albedo, especially for the Phong-type model. The models of $(\vec{N}\cdot\vec{H})$ type including the Blinn and the Ward models are significantly "darker" even after the pumping-up than the Phong-type models that converge to the ideal mirror faster by increasing n. For example, if $n = 128$, then the mean albedo of the Blinn model has been increased from 0.508 to 0.640 due to the correction. At 90 degree incident angle, on the other hand, the albedo has changed from $7.8\cdot 10^{-3}$ just to $3.7\cdot 10^{-2}$.

6.2. Ward and Schlick models

Ward [24] and Schlick [21] introduced simple BRDFs of type $(\vec{N}\cdot\vec{H})$ as simplifications of the Cook-Torrance model. These models are simpler than other known metallic models and its anisotropic form could provide particularly good metallic impression. For the isotropic case, the specular component of the Ward model has the following form:

$$f_r(\vec{L},\vec{V}) = \frac{C_{\max}}{4\pi m^2}\cdot\frac{\exp(-\tan^2\delta/m^2)}{\sqrt{((\vec{N}\cdot\vec{L})(\vec{N}\cdot\vec{V}))}}, \tag{34}$$

where $\delta = \arccos(\vec{N}\cdot\vec{H})$ and m is the standard deviation (RMS) of the surface slope.

The main problem of this model is its behavior at grazing angles and at viewing directions below the mirror direction.

© The Eurographics Association and Blackwell Publishers 1999.

Not only the BRDF but also the reflected radiance are unbounded for the Ward model, which is against practical considerations. Ward stated that selecting $C_{\max} = 1$ the model meets energy balance if $m < 0.2$. Examining the albedo function in the range of $0...89^\circ$, this is true quite accurately. Here the maximum of the albedo is greater than 0.85, and it converges to 1 if m is decreased.

However at grazing angles the albedo significantly violates energy balance (figure 5). In the next section, it will be be shown analytically that the BRDF diverges to infinity at grazing angles, thus this model is not physically plausible. For example, if $m = 0.1$, then $a(89.995^\circ) = 1.2$, $a(89.999^\circ) = 2.6$ and $a(89.9995^\circ) = 3.8$.

The previously applied modification using the $\max((\vec{N}\cdot\vec{L}),(\vec{N}\cdot\vec{V}))$ factor can also be used here, which leads to a new BRDF model:

$$f_r(\vec{L},\vec{V}) = \frac{C_{\max}}{4\pi m^2}\cdot\frac{\exp(-\tan^2\delta/m^2)}{\max((\vec{N}\cdot\vec{L}),(\vec{N}\cdot\vec{V}))}, \tag{35}$$

A similar method can be applied to the anisotropic Ward model as well.

The $C_{\max}$ constants are summarized by table 4.

m	$C_{\max}$
0.4	1.63
0.2	1.16
0.1	1.04
0.05	1.011
0.02	1.005
0.01	1.002
0.005	1.002

Table 4: *The maximum $C_{\max}$ constants for the modified Ward models (for $n < 0.05$ the $C_{\max}$ can be supposed to be 1)*

The Schlick model, on the other hand, has the following form describing the isotropic case:

$$f_r(\vec{L},\vec{V}) = \frac{C_{\max}}{4\pi}\cdot\frac{r}{(1-(1-r)(\vec{N}\cdot\vec{H})^2)^2}\cdot$$

$$\frac{1}{r+(1-r)(\vec{N}\cdot\vec{L})}\cdot\frac{1}{r+(1-r)(\vec{N}\cdot\vec{V})}, \tag{36}$$

where r determines how shiny the surface is. This model can be made physically plausible by the appropriate selection of $C_{\max}$. However, the required $C_{\max}$ factor decreases as r decreases (e.g. if $r = 0.5$, then $C_{\max} = 2.14$; if $r = 0.1$, then $C_{\max} = 0.72$; if $r = 0.01$, then $C_{\max} = 0.21$; if $r = 0.001$, then $C_{\max} = 0.042$). Thus this model becomes "dark" for usual viewing directions if r is small. The other drawback of this model is that in mirroring direction the reflected radiance can be unacceptably greater than the incoming radiance.

7. Simulation results

The following images have been rendered by a Monte-Carlo ray-tracing algorithm that incorporates the discussed importance sampling. Color computation was carried out at 8 discrete wavelengths, then using the color matching functions the XYZ primaries were generated, which were finally converted to RGB. The material properties of the metals (complex index of refraction), color matching functions and the XYZ to RGB conversion matrix were taken from [5].

The left image of figure 8 displays a golden Beethoven head of relatively low n value (4). On the other hand, the base silver plate acts as an non-perfect mirror since it has very high n value (5000) and the Fresnel function of the silver is close to 1, thus the mirror images of the other objects are just slightly blurred. The right image of figure 8 shows different metal objects on a diffuse plate. There are three point lightsources and sky-light illumination is also present.

The last two images were rendered by the plastic model of equation 30. Figure 9 shows plastic spheres on a plastic plate. All spheres have a large diffuse component defining colors of the same hue but different lightness and saturation, and the (a_s, n) specular parameters are selected according to the following sequence: $(0.04, 169)$, $(0.065, 64)$, $(0.09, 9)$, $(0.13, 3)$. Figure 10 shows two ceramic teapots. Again, the diffuse component is dominant, the n exponents are 100 and 20, respectively.

8. Conclusions

The paper derived simple and compact BRDF models from the reciprocal Phong, Blinn and Ward models, that can render metals and other specular objects. The new models are particularly suitable for importance sampling in Monte-Carlo ray-tracing algorithms. Importance sampling of the new models is simpler than that of the original Blinn and Ward models and more efficient than that of the reciprocal and non-metallic Phong model. The new model can arbitrarily well approximate the ideal mirror, thus mirrors and polishing do not require a special case.

The main advantage of the new models over existing physically based metal models is the computational time (table 5). In fact, it requires only 8 percent more computational time than the reciprocal Phong model, but its metallic impression is comparable to that of the physically based models.

© The Eurographics Association and Blackwell Publishers 1999.

BRDF model	time [min]
Phong[18]	5.4
Blinn	9.7
Ward[24]	19
Oren-Nayar[17]	35
Cook-Torrance[4]	21
He-Torrance[7]	1516
stretched Phong	5.8
stretched Blinn	10.5
modified Ward	17.6

Table 5: *Computation time of different BRDF models assuming that an* 1000×1000 *resolution image is computed using 200 samples per pixel on 8 wavelengths, and the average length of ray paths is 4. The measurements have been made on SGI Indigo 2 using Heckbert's BRDF viewer*[8]

9. Acknowledgments

The authors thank Paul Heckbert (Carnegie-Mellon) for providing his BRDF editor [8] and Eric Lafortune (Cornell) for his helpful comments. This work has been supported by the OTKA (ref.No.: F015884, T029135), the ÖAD (ref.No.: 32öu9) and the Spanish-Hungarian Fund (ref.No.: E9).

References

1. J. Arvo. Application of irradiance tensors to the simulation of non-lambertian phemomena. In *Computer Graphics (SIGGRAPH '95)*, pages 335–342, 1995.
2. P. Beckmann and A. Spizzichino. *The Scattering of Electromagnetic Waves from Rough Surfaces*. MacMillan, 1963.
3. J. Blinn. Models of light reflection for computer synthesized pictures. In *Computer Graphics (SIGGRAPH '77)*, pages 192–198, 1977.
4. R. Cook and K. Torrance. A reflectance model for computer graphics. *Computer Graphics*, 15(3), 1981.
5. A. Glassner. *Principles of Digital Image Synthesis*. Morgan Kaufmann Inc., San Francisco, 1995.
6. B. Hapke. A theoretical photometric function for the lunar surface. *Journal of Geophysical Research*, 68(15), 1963.
7. X. He, K. Torrance, F. Sillion, and D. Greenberg. A comprehensive physical model for light reflection. *Computer Graphics*, 25(4):175–186, 1991.
8. P. Heckbert. Brdf viewer, http: //www.cs.cmu.edu/ afs/ cs.cmu.edu/ user/ph/ www/src/illum. 1997.
9. D. S. Immel, M. F. Cohen, and D. P. Greenberg. A radiosity method for non-diffuse environments. In *Computer Graphics (SIGGRAPH '86)*, pages 133–142, 1986.
10. E. Ken. Reflectance phenomenology and modeling tutorial. 1994. http://www.erim.org.
11. E. Lafortune. Verbal communication. 1997.
12. E. Lafortune, S. Foo, K. Torrance, and D. Greenberg. Non-linear approximation of reflectance functions. *Computer Graphics (SIGGRAPH '97)*, pages 117–126, 1997.
13. E. Lafortune and Y. D. Willems. Using the modified phong reflectance model for physically based rendering. Technical Report RP-CW-197, Department of Computing Science, K.U. Leuven, 1994.
14. R. Lewis. Making shaders more physically plausible. In *Rendering Techniques '93*, pages 47–62, 1993.
15. M. Minnaert. The reciprocity principle in lunar photometry. *Astrophysical Journal*, 93:403–410, 1941.
16. L. Neumann, A. Neumann, and L. Szirmay-Kalos. New simple reflectance models for metals and other specular materials. Technical Report TR-186-2-98-17, Institute of Computer Graphics, Vienna University of Technology, 1998. www.cg.tuwien.ac.at/.
17. M. Oren and S. Nayar. Generalization of lambert's reflectance model. *Computer Graphics (SIGGRAPH '94)*, pages 239–246, 1994.
18. B. Phong. Illumination for computer generated images. *Communications of the ACM*, 18:311–317, 1975.
19. P. Poulin and A. Fournier. A model for anisotropic reflection. *Computer Graphics*, 24(4):273–281, 1990.
20. Ch. Schlick. A customizable reflectance model for everyday rendering. In *Fourth Eurographics Workshop on Rendering*, pages 73–83, Paris, France, 1993.
21. Ch. Schlick. An inexpensive brdf model for physically-base rendering. *Computer Graphics Forum*, 13(3):233–246, 1994.
22. L. Szirmay-Kalos. *Theory of Three Dimensional Computer Graphics*. Akadémia Kiadó, Budapest, http://www.iit.bme.hu/~szirmay.
23. K. Torrance and M. Sparrow. Off-specular peaks in the directional distribution of reflected thermal distribution. *Journal of Heat Transfer — Transactions of the ASME*, pages 223–230, May 1966.
24. G. Ward. Measuring and modeling anisotropic reflection. *Computer Graphics*, 26(2):265–272, 1992.

© The Eurographics Association and Blackwell Publishers 1999.

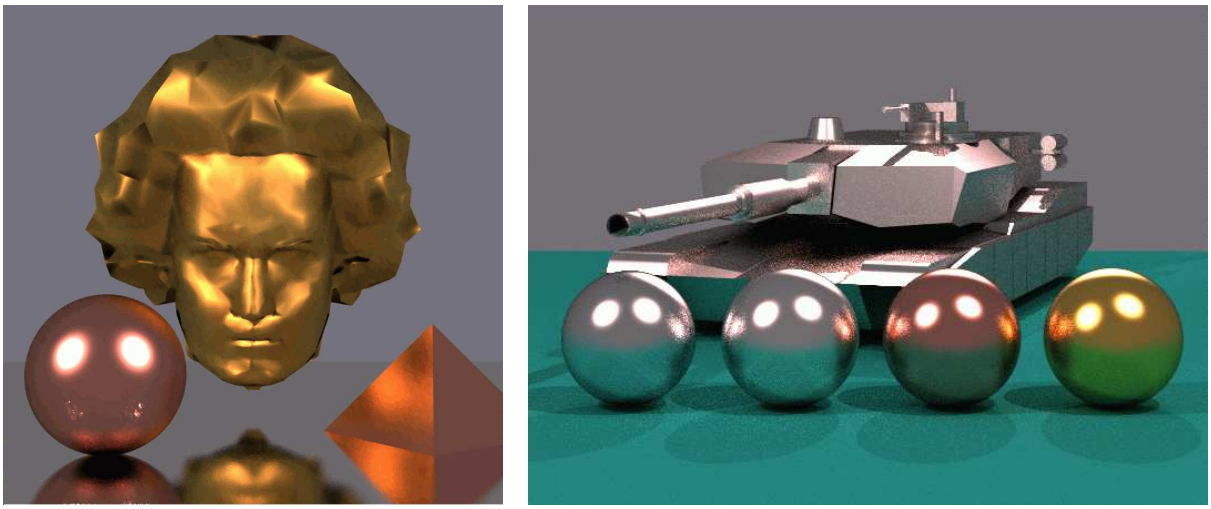

Figure 8: *Left: a golden Beethoven ($n = 4$) with a copper sphere ($n = 40$) and a copper pyramid ($n = 150$) on a silver mirror ($n = 5000$); Right: a silver tank ($n = 20$) with aluminum ($n = 40$), silver ($n = 50$), copper ($n = 50$) and golden ($n = 40$) spheres*

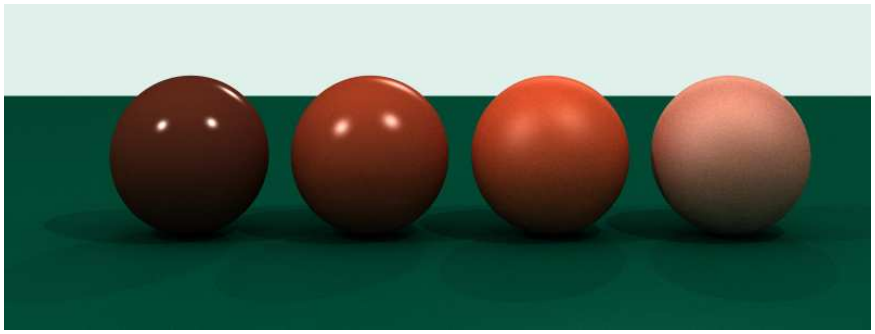

Figure 9: *Plastic objects*

Figure 10: *Ceramic teapots*

© The Eurographics Association and Blackwell Publishers 1999.